



Shahid Chamran  
University of Ahvaz

# Journal of Applied and Computational Mechanics



Research Paper

## Performance Investigation of Simple Low-dissipation AUSM (SLAU) Scheme in Modeling of 2-D Inviscid Flow in Steam Turbine Cascade Blades

Fahimeh Ebrahimzadeh Azghadi<sup>1</sup>, Mahmoud PasandidehFard<sup>2</sup>, Mohammad Reza Mahpeykar<sup>3</sup>

<sup>1</sup> Department of Mechanical Engineering, Ferdowsi University of Mashhad, Mashhad, Iran, Email: ebrahimzadeh.f2@gmail.com

<sup>2</sup> Department of Mechanical Engineering, Ferdowsi University of Mashhad, Mashhad, Iran, Email: fard\_m@um.ac.ir

<sup>3</sup> Department of Mechanical Engineering, Ferdowsi University of Mashhad, Mashhad, Iran, Email: mahpeymr@um.ac.ir

Received January 30 2021; Revised May 09 2021; Accepted for publication May 10 2021.

Corresponding author: M. PasandidehFard (fard\_m@um.ac.ir)

© 2021 Published by Shahid Chamran University of Ahvaz

**Abstract.** This study evaluates the performance of the SLAU, AUSM+UP upwind schemes, and CUSP artificial dissipation scheme for the flow through the convergent-divergent nozzles and turbine stator blades under different pressure ratios by developing an in-house code. By comparing the results with analytical and experimental results, it is found that, despite the simplicity of the SLAU scheme in the absence of tuning variables, it provides reasonable predictions for different turbine blades in point of location and strength of the shocks. The SLAU scheme could converge at a much higher rate, leading to very much lower values of residuals. The SLAU scheme causes about 30% and 20% improvements over the prediction of the shock-induced losses in supersonic and subsonic outlet flows, respectively.

**Keywords:** Upwind Scheme; AUSM+UP; SLAU; Turbine Blade; Artificial Dissipation.

### 1. Introduction

Turbines are essential elements in different industrial applications. Effective design to improve the turbine efficiency requires a true understanding of the flow characteristics as it passes through the turbine blades (Fig. 1). In recent years, different numerical methods have been proposed to numerical modeling of the flow between turbine blades and calculating the associated losses and errors. The achievement of an accurate numerical method with minimum computation and numerical errors for modeling the flow in a wide range of regimes has always been of interest to researchers in the field of computational fluid dynamics.



Fig. 1. Cascade schematic of a steam turbine blade



In numerical methods, to simulate the flows accurately, the governing equations discretized with the higher accuracy discretization schemes, which are unstable with numerical fluctuations. To reduce or eliminate these oscillations, there are two methods, classical and modern methods. In the classical method, to reduce or eliminate these oscillations, artificial dissipations add to the equations, but they are not completely eliminated [1]. In modern methods such as NVD2 [2], TVD1 [3], and WENO4 [4], by applying flux limiters to the equations, numerical fluctuations are completely terminated.

In other way, numerical methods can be broadly classified under two classes, namely central difference schemes (or artificial dissipation schemes) and upwind schemes. In 1995, the basis of the artificial dissipation scheme initiated by Jameson in which an adaptive blend of fourth-order and second-order dissipative terms added to the equations as artificial dissipation terms. In an artificial dissipation scheme, it is a crucial task to determine the dissipation appropriately, because excessive dissipation leads to a sharp gradient. Accordingly, Jameson proposed the CUSP (Convective Upstream Split Pressure) scheme, in which a switching function was utilized to detect the flow [5].

Upwind schemes that have now become the primary spatial discretization technique are in harmony with the physics of the flow across the domain. Liou [6] developed the AUSM (Advection Upstream Splitting Method) scheme, which is based on splitting the flux to pressure and convective terms separately. The convective terms are upstream-based and are convected by a cell-interface velocity. In contrast, acoustic wave speeds govern the pressure flux terms.

In recent years, to increase accuracy and reduce numerical diffusion of the original AUSM scheme, different versions of AUSM-family schemes with several capabilities and weaknesses have been proposed [7]. Furthermore, to precisely predict problems containing a wide range of flow regimes – from incompressible to highly compressible flow regions in the same computational domain, accurate and robust numerical scheme capable of modeling all-speed flow is required. In 2006, to enhance the efficiency of schemes in low Mach number flow, Liou [8] modified AUSM-family schemes and developed a new scheme, named the AUSM+UP. AUSM+UP scheme is reliable and executable over a wide range of Mach numbers. However, it has several problem-dependent parameters, and the modification slightly spoils the simplicity of the original AUSM scheme [9].

These schemes have been used for turbine blades in many publications. Fort et. al [10] proposed a proper numerical approximation of boundary conditions for the flow field in a turbine cascade. Their Numerical simulations were based on the Favre-averaged Navier–Stokes equations with SST  $k-\omega$  turbulence model and the in-house implicit finite volume solver with AUSM-type discretization. Loda et. al [11] presented mathematical models for inviscid and also viscous transonic flows through turbine cascades. The flux splitting methods in their study include AUSM, AUSMPW+, and HLLC Riemann solvers. In another study, Loda et. al [12] investigated the numerical simulation of turbulent flow through turbine cascades including heat exchange between fluid and blades. The numerical algorithm couples an implicit AUSM finite volume solver for fluid flow and a finite element solver for heat conduction inside the blade. Pacciani et. al [13] compared the AUSM+UP scheme with two other numerical flux schemes in the framework of a RANS/URANS code for turbomachinery applications. The considered advection schemes include central discretizations with artificial dissipation and the Roe upwind scheme. Alakashi and Basuno [14] employed the Cell-centered scheme, Roe Upwind Scheme, and TVD Scheme to investigate the inviscid compressible flow pass through a two-dimensional blade on two types of blade shapes. Singh and Holmes [15], considering the HCUSP artificial dissipation schemes are more amenable to implementation in central difference codes than the AUSM family of schemes, but AUSM family of schemes has several attractive properties over H-CUSP. Thus they proposed AD-AUSM scheme to signify a hybrid of artificial dissipation and AUSM family of schemes. The tests showed that AD-AUSM can capture contact waves with the accuracy of AUSM schemes. It is more robust and performs better across shocks than the H-CUSP variant. It is more dissipative across shocks than AUSM+UP and AUSMPW+ schemes but has a smoother behavior across sonic transition points.

Recently, despite the high accuracy and efficiency of AUSM-family schemes, Shima and Kitamura [16] also modified AUSM-family schemes and developed an all-speed scheme, called the SLAU (Simple low-dissipation AUSM family scheme). Although several all-speed schemes have been developed, however, these schemes contain at least one reference parameter. Simplicity is the main property of the SLAU scheme, and it includes no parameter to be tuned, such as the cut-off Mach number in the AUSM+UP scheme [17]. The SLAU scheme has low dissipation in the low Mach number region, and maintains robustness at high Mach numbers flow [18].

In the present research, first, the equations of SLAU and AUSM+UP upwind schemes and CUSP artificial dissipation scheme are briefly reviewed. Then, by developing in-house code, to validate the AUSM family upwind schemes in different Mach number regimes, the results of SLAU, AUSM + UP, and CUSP schemes for a one-dimensional, adiabatic and inviscid flow in two convergent-diverging nozzles under three pressure ratios are presented and compared with the results of the analytical solutions. In steam turbine blades usually, several subsequent shock waves occurred which get weak respectively. The prediction of location and strength of these shocks is a challenge which is considered in this article. Afterward, the performance of AUSM+UP and SLAU upwind schemes in two-dimensional, single-phase, and inviscid flow between steam turbine stator blades is examined. Also, the results of AUSM+UP, SLAU, and CUSP schemes are compared with the available experimental results on two types of mid-section and tip section turbine blades under various outlet conditions.

## 2. Numerical Schemes

As mentioned before, the numerical methods classified under central difference schemes and upwind schemes. The central difference schemes are based on an equal contribution of the flow information saved at points beside the cell surfaces. In other words, these schemes disregard the direction in which the information reaches the cell and ignore the nature of the problems. In these schemes, to inhibit possible oscillations in the solution, an appropriate approximation of the terms omitted during the discretization stage is added to the equations in the form of artificial dissipation, which causes some error.

Upwind schemes are based on the propagative characteristic of waves and categorize into two types of flux difference splitting and flux vector splitting methods. Nowadays, the development of upstream methods is motivated by the tendency to combine both the precision of the flux difference splitting methods and the capabilities of the flux vector splitting methods. In these schemes, to determine convective velocity and pressure on the cell face, polynomial functions are used. In this paper, the three widely used schemes in recent years are considered.

### 2.1 AUSM+UP

As already mentioned, in all AUSM-family schemes, the inviscid flux is split into pressure and convective fluxes. Therefore, the inviscid flux at the cell interface has the form of [19]

$$\vec{F}_{1/2} = \dot{m}_{1/2} \vec{\psi}_{L/R} + \vec{p}_{1/2} \quad (1)$$



where

$$\vec{\psi}_{L/R} = \begin{cases} \vec{\psi}_L & \dot{m}_{1/2} > 0 \\ \vec{\psi}_R & \text{otherwise} \end{cases} \tag{2}$$

$$\vec{p}_{1/2} = p_{1/2} \begin{bmatrix} 0 & \vec{n}_x & \vec{n}_y & 0 \end{bmatrix}^T \tag{3}$$

$$\vec{\psi}_{L/R} = [1, \vec{u}_{L/R}, \vec{v}_{L/R}, H_{L/R}] \tag{4}$$

where  $p_{1/2}$  is the cell interface pressure. In the AUSM family schemes the cell interface mass flux is defined differently. In this scheme, the cell interface mass flux is signified by subscript "1/2".

$$\dot{m}_{1/2} = a_{1/2} M_{1/2} \rho_{L/R} \tag{5}$$

where

$$\rho_{L/R} = \begin{cases} \rho_L & q_{1/2} > 0 \\ \rho_R & \text{otherwise} \end{cases} \tag{6}$$

where  $\rho_{1/2}$  is the density convected by the convective velocity  $q_{1/2}$  ( $q$  is the velocity component normal to the cell face). The subscripts "L" and "R", respectively, refer to the left and right cells of the cell interface. It is more straightforward to utilize the Mach number as a working variable. So, rewriting the above equation gives [8]:

$$\dot{m}_{1/2} = a_{1/2} M_{1/2} \begin{cases} \rho_L & M_{1/2} > 0 \\ \rho_R & \text{otherwise} \end{cases} \tag{7}$$

The "UP" suffix in the AUSM+UP scheme is justified that "U" signifies the velocity diffusion term in the cell interface pressure equation, and "P" signifies the pressure diffusion term in the equations of the cell interface Mach number. The cell interface Mach number in terms of  $M_L$  and  $M_R$  defined as [8]:

$$M_{1/2} = M_m^+(M_L) + M_m^-(M_R) + M_p \tag{8}$$

where  $M_m$  are the polynomial functions of degree  $m$  ( $m=1,2, 4$ ) [19]. In the present work, the 4th-degree polynomial function is used that is expressed as:

$$M_4^\pm = \begin{cases} \frac{1}{2}(M \pm |M|) & \text{if } |M| \geq 1 \\ \pm \frac{1}{4}(M \pm 1)^2 (1 + 4\beta(M \mp 1)^2) & \text{otherwise} \end{cases} \tag{9}$$

In the above equation  $\beta = 1/8$ . As mentioned above, to improve computations in the low Mach number regions, the pressure diffusion term,  $M_p$ , is added.

$$M_p = -\frac{K_p}{f_a} \max(1 - \sigma \bar{M}^2, 0) \frac{P_R - P_L}{\rho_{1/2} a_{1/2}^2} \tag{10}$$

$$\rho_{1/2} = \frac{\rho_L + \rho_R}{2}, \quad \sigma \leq 1, 0 \leq K_p \leq 1$$

Different equations have been suggested for the scaling factor  $f_a$ . In this study, the simplest one has been used.

$$f_a(M_o) = M_o(2 - M_o) \tag{11}$$

where the reference Mach number is:

$$M_o^2 = \min(1, \max(\bar{M}^2, M_{co}^2)) \tag{12}$$

The cut-off Mach number  $M_{co}$  is indicated as  $O(M_\infty)$  and should avoid becoming zero. The mean local Mach number is given by:

$$\bar{M}^2 = \frac{1}{2}(M_L^2 + M_R^2) \tag{13}$$

Velocity diffusion term,  $P_u$ , also is added to enhance computations in the low Mach number regions and is used to develop a scheme for all speeds. The interface pressure formula is defined as:

$$p_{1/2} = P_n^+(M_L)P_L + P_n^-(M_R)P_R + P_u \tag{14}$$

$$P_u = -2k_u P_5^+(M_L)P_5^-(M_R)\rho_{1/2}f_a a_{1/2}(u_R - u_L) \quad 0 \leq k_u \leq 1 \tag{15}$$

It also can be written as below:

$$p_{1/2} = \frac{P_L + P_R}{2} + \frac{P_n^+(M_L) - P_n^-(M_R)}{2}(P_L - P_R) + (P_n^+(M_L) + P_n^-(M_R) - 1)\frac{P_L + P_R}{2} + P_u \tag{16}$$



where  $n = 1, 3,$  or  $5$  corresponds to the degree of the polynomials  $P^\pm$ . It is found that the fifth-degree polynomials are chosen to provide more accurate solutions [8].

$$P_5^\pm(M) = \begin{cases} \frac{1}{2M}(M \pm |M|) & \text{if } |M| \geq 1 \\ \pm \frac{1}{4}(M \pm 1)^2 \left[ (\pm 2 - M) \mp 16\alpha M \left( \mp \frac{1}{4}(M \mp 1)^2 \right) \right] & \text{otherwise} \end{cases} \quad (17)$$

In the AUSM+UP scheme, the user has no role in choosing the uncertain coefficient  $\alpha$ , as this parameter is intelligently entered into the equations using the following formula.

$$\alpha = \frac{3}{16}(-4 + 5f_a^2) \in \left[ -\frac{3}{4}, \frac{3}{16} \right] \quad (18)$$

In AUSM+UP scheme, the interface speed of sound is defined as [20]:

$$a_{1/2} = \min(\hat{a}_L, \hat{a}_R) \quad (19)$$

where

$$\hat{a}_L = (c^*)^2 / \max(c^*, u_L) \quad (20)$$

$$\hat{a}_R = (c^*)^2 / \max(c^*, -u_R) \quad (21)$$

$$(c^*)^2 = \frac{2(\gamma - 1)}{\gamma + 1} H \quad (22)$$

As can be seen in this method, there are several dependent-parameters, as  $K_u, K_p$ , and  $\sigma$ , for calculating Mach number and pressure on the cell surface. The values of these parameters vary in different flow regimes and depend on the type of flow. Generally,  $K_u$  and  $K_p$  are proposed to be 0.75 and 0.25, respectively [13]. So, it can be problematic since there is no convenient method to specify these parameters, especially when there is no uniform flow.

## 2.2 SLAU

Recently, a simple low-dissipation numerical flux of the AUSM-family, named SLAU, has been devised for a wide range of regimes. This scheme differs from the AUSM + UP scheme in defining pressure flux. The new cell interface pressure equation is given by:

$$p_{1/2} = \frac{P_L + P_R}{2} + \frac{P_n^+(M_L) - P_n^-(M_R)}{2}(P_L - P_R) + f_p(P_n^+(M_L) + P_n^-(M_R) - 1) \frac{P_L + P_R}{2} \quad (23)$$

To control the dissipation value while keeping stability, the nondimensional function,  $f_p$ , is used in this term. For this purpose, it should have the following characteristic.

$$f_p = \begin{cases} \propto |M| & |M| < 1 \\ = 1 & |M| \geq 1 \end{cases} \quad (24)$$

A simple form for this function is proposed as:

$$f_p = (1 - \chi), \quad \chi = \left(1 - \hat{M}\right)^2 \quad (25)$$

$$\hat{M} = \min\left(1, \frac{1}{c} \sqrt{\frac{u^{+2} + v^{+2} + u^{-2} + v^{-2}}{2}}\right) \quad (26)$$

Furthermore, for the local Mach number definition, the normal component and free-stream Mach number are employed in the AUSM+UP scheme, whereas, in this scheme, multidimensional velocity is used without any reference parameter. It is noteworthy that this amendment does not affect the nature of contact discontinuity preserving. [21]. In contrast with other all-speed schemes, the SLAU scheme is an all-speed scheme that is free from the problem-dependent parameters; therefore, its broad applicability is expected.

## 2.3 CUSP

This scheme is based on the dissociation of the pressure terms in the flux equations [22]. The components of the flux vector in two-dimensional flow are expressed by:

$$\vec{F} = \vec{F}_x \cdot S_y + \vec{F}_y \cdot S_x \quad (27)$$

$S_x$  and  $S_y$  are the surface borders in the  $x$  and  $y$  directions, respectively. The flow flux is split into two components, convective and pressure terms as [15]:

$$\vec{F}_x = u \cdot \vec{w} + \vec{F}_{px}, \quad \vec{F}_y = v \cdot \vec{w} + \vec{F}_{py}, \quad (28)$$



where  $w$  contains the two-dimensional flow conservation variables and pressure vector in  $x$  and  $y$  directions is given by:

$$\vec{w} = \begin{bmatrix} \rho \\ \rho.u \\ \rho.v \\ \rho.e \end{bmatrix}, \quad \vec{F}_{py} = \begin{bmatrix} 0 \\ 0 \\ p \\ u.p \end{bmatrix}, \quad \vec{F}_{px} = \begin{bmatrix} 0 \\ p \\ 0 \\ u.p \end{bmatrix} \tag{29}$$

As mentioned before the flow flux contains convective and pressure terms and the dissipation term that adds to the flux vector is defined as follows:

$$\vec{F}_{i+1/2} = \frac{\vec{F}_i + \vec{F}_{i+1}}{2} - d_{i+1/2} \tag{30}$$

or

$$\vec{F}_{i+1/2} = \frac{\vec{F}_i^c + \vec{F}_{i+1}^c}{2} + \left( \frac{F_i^p + F_{i+1}^p}{2} \right) - d_{i+1/2} \tag{31}$$

$$d_{i+1/2} = \frac{1}{2} \alpha_{i+1/2} \dot{c} (w_{i+1} - w_i) + \frac{1}{2} \beta_{i+1/2} (F_{i+1} - F_i) \tag{32}$$

$$\alpha \dot{c} = \alpha c - \beta \bar{u} \tag{33}$$

where  $\alpha$  and  $\beta$  defined as follows [23, 24]:

$$\alpha = \begin{cases} |M| & \text{for } |M| > 0.0001 \\ \frac{1}{2} \left( \alpha_0 + \frac{|M|}{\alpha_0} \right) & \text{others} \end{cases} \tag{34}$$

$$\beta = \begin{cases} \max(0, 2M - 1) & 0 \leq M \leq 1 \\ \min(0, 2M + 1) & -1 \leq M \leq 0 \\ \text{sign}(M) & |M| > 1 \end{cases} \tag{35}$$

Artificial dissipation should be added with high values adjacent to shock waves and low values in the rest of the solution domain, to obtain more precise results. For this purpose, a switch function,  $L(u,v)$ , which has a fundamental role in the convergence of the solution and is capable of flow detection, is used in the computations [22].

$$L(u,v) = \frac{1}{2} \left( 1 - \left| \frac{u-v}{|u|+|v|} \right|^q \right) (u+v) \tag{36}$$

The value of the power  $q$  is selective and between 2 and 3 [25]. Now,  $w_{i+1}$  and  $w_i$  should be replaced by a variable vector at right and left- hand sides.

$$w_R = w_{i+1} - \frac{1}{2} L(\Delta w_{i+3/2}, \Delta w_{i-1/2}) \tag{37}$$

$$w_L = w_i + \frac{1}{2} L(\Delta w_{i+3/2}, \Delta w_{i-1/2}) \tag{38}$$

#### 2.4 Comparison of pressure flux in AUSM family schemes

The following equation is used to calculate the pressure on the cell interface in all AUSM family methods [18]:

$$p_{1/2} = P_n^+(M_L)P_L + P_n^-(M_R)P_R \tag{39}$$

or

$$p_{1/2} = \frac{P_L + P_R}{2} + \frac{P_n^+(M_L) - P_n^-(M_R)}{2} (P_L - P_R) + (P_n^+(M_L) + P_n^-(M_R) - 1) \frac{P_L + P_R}{2} \tag{40}$$

For supersonic flows with substituting the  $P^*$  from the above equation:

$$p_{\frac{1}{2}} = \frac{P_L + P_R}{2} + \frac{1-0}{2} (P_L - P_R) + (1+0-1) \frac{P_L + P_R}{2} = \frac{P_L + P_R}{2} + \frac{1}{2} (P_L - P_R) = p_L \tag{41}$$

As can be seen, the first dissipative term in eq. (40), which is proportional to the pressure difference, changes from the central difference state to the upwind state, and the second dissipative term, which corresponds to the average pressure of the two cells is also disappeared. Accordingly, the flux is fully upwind.

Also, for subsonic flows with a Mach number much smaller than one regardless of the higher-order terms with substituting the  $\beta^*$ :



$$p_{\frac{1}{2}} = \frac{P_L + P_R}{2} + \left(\frac{3}{4} + \alpha\right) \frac{M_L + M_R}{2} (P_L - P_R) + \left(\frac{3}{4} + \alpha\right) \frac{P_L + P_R}{2} (M_L - M_R) = \frac{P_L + P_R}{2} + \left(\frac{3}{4} + \alpha\right) (P_L M_L - P_R M_R) \quad (42)$$

As can be seen, the first and second dissipative terms in eq. (40) for subsonic flows have been merged into one term.

The first term in eq. (40) in calculating the pressure flux, even at low Mach, results in severe fluctuations and even divergence. So, it has been reduced in the SLAU scheme to control the dissipation and removed in the AUSM+UP scheme, and another term is introduced.

According to eq. (14) the AUSM+UP scheme has an additional dissipation term controlled by the function  $f_a$ , which also asymptotes to  $2M$  at low speeds [26].

In the SLAU scheme, the second term of dissipation is scaled with a function that is of local Mach number, in other words, a scale of convective terms is included in the calculation of the pressure flux. This function is considering the multidimensional Mach number. They showed in eqs. (23 - 26) [27].

### 3. Results

As explained in the introduction, in this research, the performance of SLAU, AUSM+UP upwind schemes, and the CUSP artificial dissipation scheme for one-dimensional, adiabatic, and inviscid flow in the convergent-divergent nozzles is evaluated and compared with the analytical solution. In this section, the three different pressure ratios is considered for examining the ability of the above schemes in a wide range of Mach number such as transonic flow and the flow which has a wide range of Mach number from subsonic to supersonic. In the following sections, the three schemes are applied for modeling the two-dimensional, adiabatic, and inviscid flow between turbine blades. The comparison between these schemes is carried out by studying two types of turbine blades, namely tip-section and mid-section, under two expansion ratios.

#### 3.1 Convergent-Divergent Nozzle

Figure 2 shows the geometry of the convergent-divergent nozzle, which has an area ratio of 1.5. The computational grid is a standard mesh, and it has 200 cells in x-direction where independence of the solution from the grid system is verified. The following equation defines the profile equation of the nozzle.

$$y = 0.25x^2 + 0.5 \quad (43)$$

Assuming the amount of 0.7 for pressure ratio (back pressure to the stagnation pressure), the value of Mach number starts from about 0.77 at the nozzle inlet. By decreasing the area, the Mach number increases to about 1.7 adjacent to the outlet, then a normal shock wave occurs. Mach number distribution along the nozzle obtained from SLAU, AUSM+UP and CUSP schemes along with the analytical solution is illustrated in Fig. 3. As it is shown, the three methods apparently provide acceptable results, but from a closer view to the shock region (before and after the shock), there are some differences in predicting the location and strength of shock wave.

Also, the position of the shock wave, the Mach number values before and after the shock wave, and the stagnation pressure drop regarding the predictions of these schemes are presented in Table 1 and compared with the analytical solution obtained from thermodynamic tables. The stagnation pressure drop due to aerodynamic shocks is calculated from the below equation.

$$\frac{P_{02}}{P_{01}} = \left[ \frac{(\gamma + 1)M^2}{(\gamma - 1)M^2 + 2} \right]^{\gamma/(\gamma-1)} + \left[ \frac{(\gamma + 1)}{2\gamma M^2 - (\gamma - 1)} \right]^{1/(\gamma-1)} \quad (44)$$

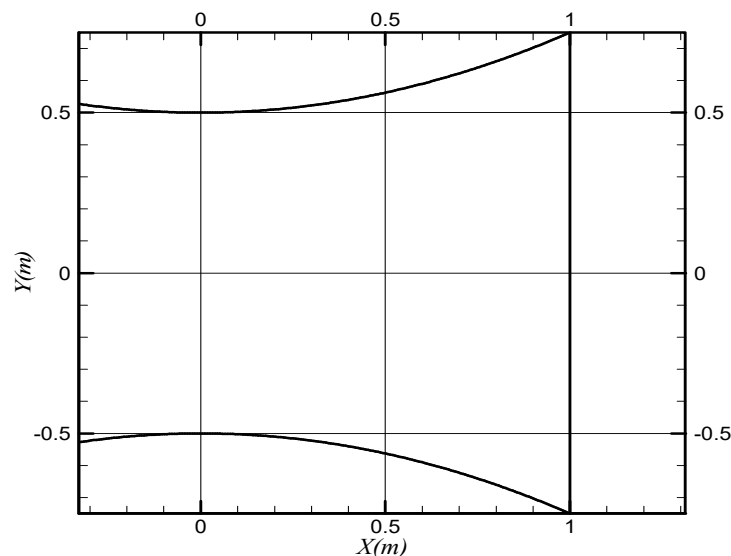


Fig. 2. Geometry of the convergent-divergent nozzle (pressure ratio=0.7 and 0.87)



**Table 1.** Comparison of calculated shock wave parameters with the analytical solution (pressure ratio=0.7)

Schemes	Dynamic gas table	AUSM+UP	CUSP	SLAU
Starting point of the shock (m)	0.8343	0.8348	0.8348	0.8348
Position of the end of the shock (m)	0.834	0.841	0.847	0.847
$M_1$	1.711	1.710	1.717	1.712
$M_2$	0.6377	0.6423	0.6345	0.6367
$P_{02}/P_{01}$	0.851	0.849	0.842	0.849

Table 1 and Fig. 3 show that the analytical solution leads to the shock position at  $x=0.834$ , assuming the amount of 0.7 for the pressure ratio. As can be seen, the shock position and the Mach number before and after the shock wave by applying the SLAU scheme is predicted better than two other schemes. Furthermore, the predicted shock thickness, obtained by the SLAU scheme, is the least one, and so preferable. According to this figure and Table 1, it is clear that the SLAU scheme generally captures the shock more accurately.

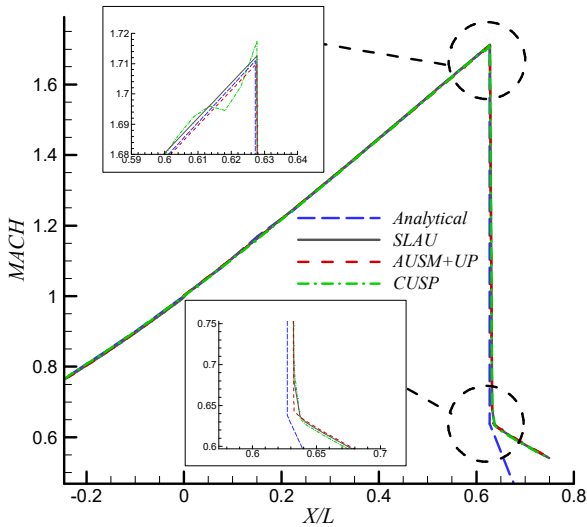


**Fig. 3.** Distribution of Mach number along the nozzle and before and after shock (pressure ratio=0.7)

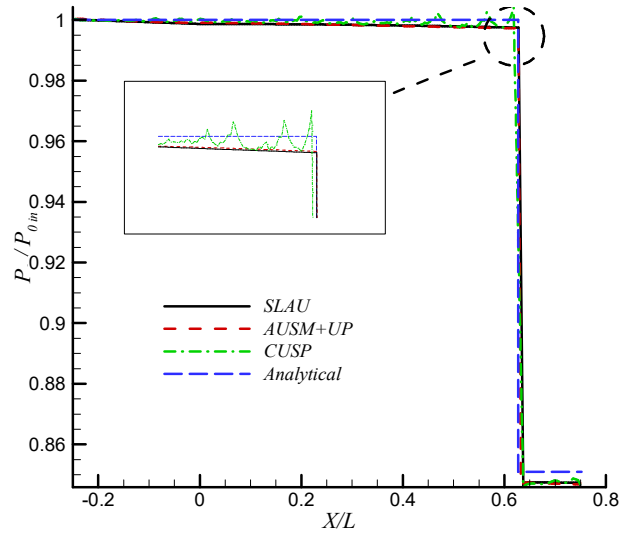


**Fig. 4.** Distribution of stagnation pressure to inlet stagnation pressure in the nozzle (pressure ratio=0.7)

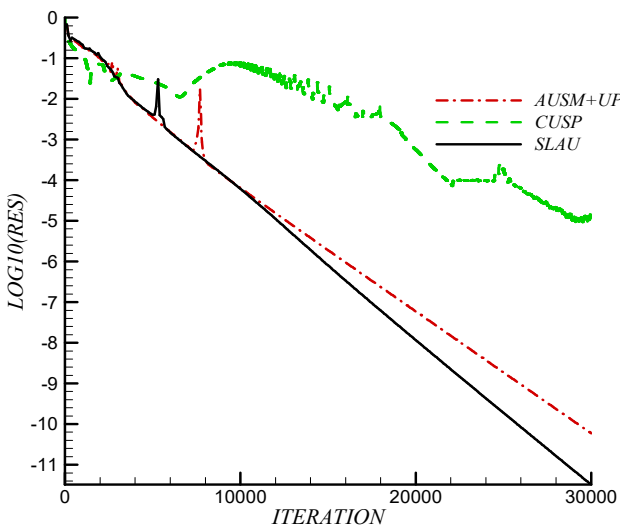


**Fig. 5.** Variation of logarithmic residual (pressure ratio=0.7)

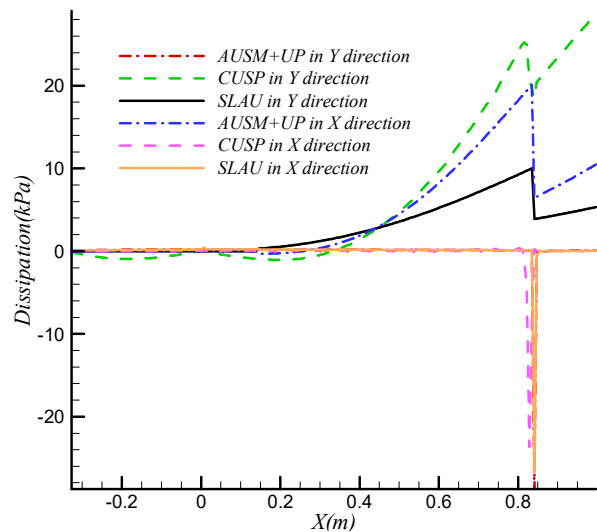


**Fig. 6.** Pressure dissipation term of the SLAU and AUSM+UP schemes and total dissipation of the CUSP scheme in x and y directions along the nozzle (pressure ratio=0.7)





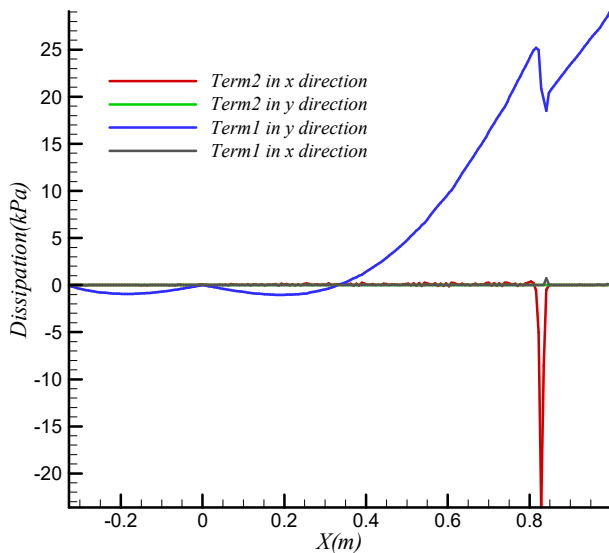


Fig. 7. Distribution of the components of artificial dissipation in CUSP scheme in the x and y direction (term1: convection and term2: pressure), (pressure ratio=0.7)

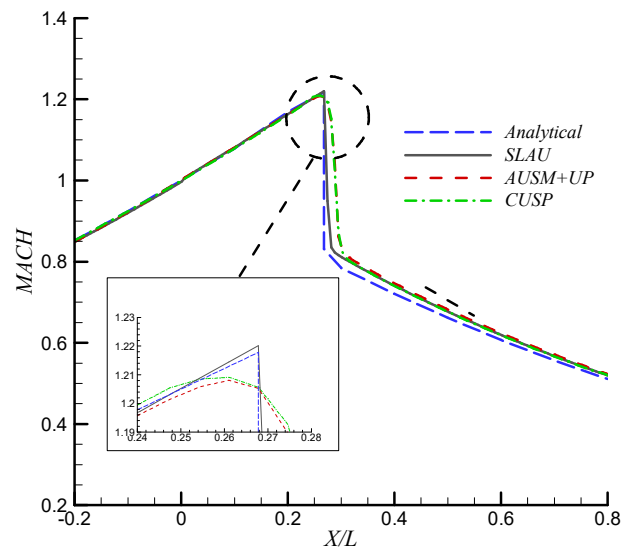


Fig. 8. Distribution of Mach number along the nozzle (pressure ratio=0.87)

The shock-induced losses in calculations are represented by decreasing in the stagnation pressure. In the conducted adiabatic and inviscid modeling, the stagnation pressure must remain constant until the shock wave; and drops at the shock location. The closer this drop to the value calculated in the analytical solutions, denote suitable agreement with the pre-assumptions. The changes of stagnation pressure to the inlet stagnation pressure of the nozzle obtained from the three mentioned schemes and the stagnation pressure drop by the analytical solution are shown in Fig. 4. As can be seen from this figure and table 1, the CUSP scheme has fluctuations near the shock, and the SLAU and AUSM+UP schemes estimated the stagnation pressure better than the CUSP scheme.

Figure 5 illustrates the convergence rate in terms of the number of iterations for the three mentioned schemes. The convergence speed depends on the CFL number, which in this study is equal to 0.5 for all schemes. As shown in Fig. 5 the SLAU scheme converges at a much higher rate due to less computing. So, the SLAU upwind scheme needs fewer iterations to achieve specific residual than the other two methods. Also, this scheme leads to very much lower values of residuals compared with the CUSP artificial dissipation scheme.

Figure 6 shows the pressure dissipation term in the SLAU, AUSM+UP schemes, and total dissipation term in the CUSP scheme in x and y directions. It can be seen, the SLAU scheme applies the lowest amount of dissipation and the CUSP scheme applies the greatest amount of dissipation. Although the CUSP scheme applies the lower amount of dissipation in the x-direction, it applies artificial dissipation in a larger region; so, it applies more dissipation. As mentioned before excessive dissipation leads to errors in the numerical solution.

Equations (47) and (48) are the dissipation term for the CUSP scheme in x and y directions, which are obtained by substituting the conservative variables and flux terms for the momentum equation in x and y directions in eq. (32). The equation of the pressure dissipation according to AUSM+UP and SLAU schemes which respectively obtained from eqs. (16), (23), are as follows:

$$D_{p,SLAU} = \frac{P_n^+(M_L) - P_n^-(M_R)}{2} (P_L - P_R) + (1 - \chi) (P_n^+(M_L) + P_n^-(M_R) - 1) \frac{P_L + P_R}{2} \tag{45}$$

$$D_{p,AUSM+UP} = \frac{P_n^+(M_L) - P_n^-(M_R)}{2} (P_L - P_R) + (P_n^+(M_L) + P_n^-(M_R) - 1) \frac{P_L + P_R}{2} + P_u \tag{46}$$

$$D_{CUSP} = D_p + D_c = \frac{1}{2} \alpha_{i+1/2}^* c (\rho u_{i+1} - \rho u_i) + \frac{1}{2} \beta_{i+1/2} \left( (\rho u^2 + p)_{i+1} - (\rho u^2 + p)_i \right) \tag{47}$$

$$D_{CUSP} = D_p + D_c = \frac{1}{2} \alpha_{i+1/2}^* c (\rho v_{i+1} - \rho v_i) + \frac{1}{2} \beta_{i+1/2} \left( (\rho v^2 + p)_{i+1} - (\rho v^2 + p)_i \right) \tag{48}$$

The artificial dissipation term in the CUSP scheme contains two terms, convection, and pressure which are applied to the flux term totally. Further, the distribution of the components of dissipation in the CUSP scheme in the x and y direction are shown in Fig. 7. As can be seen from Fig. 7, the role of the first term (convection) of the artificial dissipation equation can be neglected and in y-direction, the role of the second term (pressure) is equal to zero.

Considering the pressure ratio equal to 0.87, which leads to the transonic flow, a weak shock wave occurred in the nozzle. The position of the shock wave, the Mach number values before and after the shock wave, and the stagnation pressure drop obtained by AUSM+UP and SLAU and CUSP schemes are presented in table 2 and compared with the analytical solution obtained from thermodynamic tables. Also, the distribution of Mach number along the nozzle obtained by SLAU, AUSM+UP and CUSP schemes and the analytical solution is illustrated in Fig. 8. In this pressure ratio, the flow is transonic and the value of the Mach number is about 1.2 near the normal shock. The SLAU scheme performance in predicting the position and strength of shock is better than two other schemes and the thickness of the shock by the SLAU scheme is at least.





**Table 2.** Comparison of calculated shock wave parameters with the analytical solution (pressure ratio=0.87)

Schemes	Dynamic gas table	AUSM+UP	CUSP	SLAU
Starting point of the shock (m)	0.2678	0.2616	0.2616	0.2677
the shock (m) end of of the Position	0.2678	0.3017	0.3017	0.2819
$M_1$	1.2178	1.2078	1.2088	1.2201
$M_2$	0.8313	0.8323	0.8262	0.8346
$P_{02}/P_{01}$	0.99097	0.9879	0.9870	0.9889

The stagnation pressure drop due to the normal shock is shown in Fig. 9. As can be seen, the CUSP scheme has high fluctuations near the shock, and from the comparison of the results with the analytical solutions, the SLAU scheme estimated the pressure drop more closer to the value calculated in the analytical solutions than others, which denotes suitable agreement with the pre-assumptions. So, the SLAU scheme in addition to simplicity- due to non-existing any tunable parameter, and a high rate of convergence- simulated the flow in the transonic regime better than AUSM+UP and CUSP schemes.

Further, in the nozzles with a wide range of the Mach number from subsonic to supersonic in the same computational domain, an accurate and robust numerical scheme is needed to predict all-speed flows precisely. Considering a nozzle with an area ratio of 8.2 and the pressure ratio of 0.35, the Mach number changes from about 0.5 at the inlet to 3 near the shock. Figure 10 shows the considered nozzle.

The distribution of Mach number estimated by SLAU and AUSM+UP upwind schemes and the CUSP artificial scheme is shown in Fig. 11. By comparing the results with the analytical solution, in point of the location and strength of the shock and stagnation pressure drop, which are presented in table 3 it is observable, that the SLAU scheme has a great ability to predict all regimes. While in the CUSP scheme result some fluctuations are seen around the shock, and the AUSM+UP has dependent variables that should be tuned in different regimes to find the suitable values.

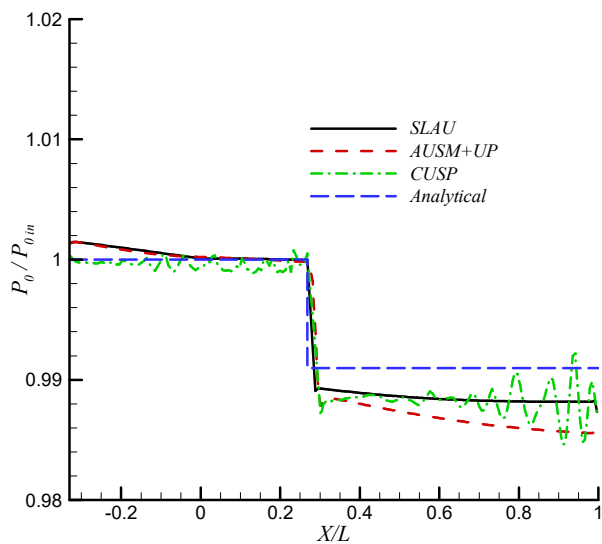


**Fig. 9.** Distribution of stagnation pressure to inlet stagnation pressure in the nozzle (pressure ratio=0.87)

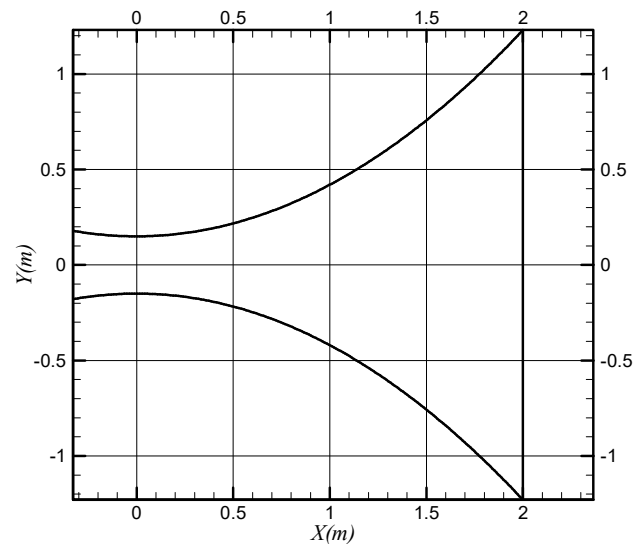


**Fig. 10.** Geometry of the convergent-divergent nozzle (pressure ratio=0.35)

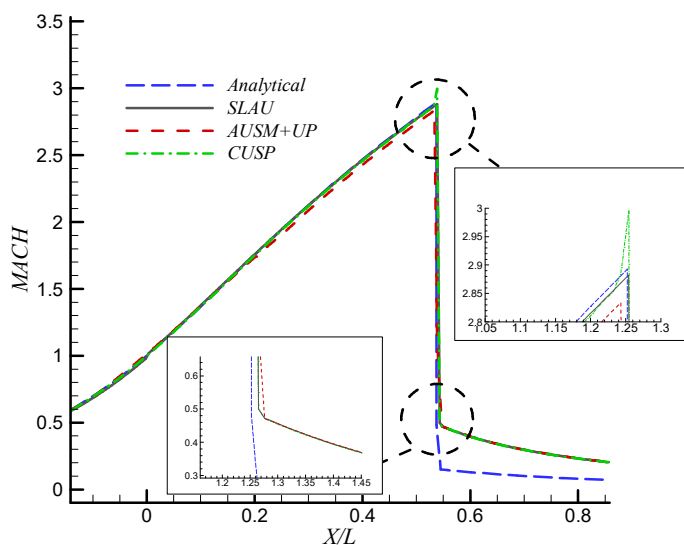


**Fig. 11.** Distribution of Mach number along the nozzle (pressure ratio=0.35)

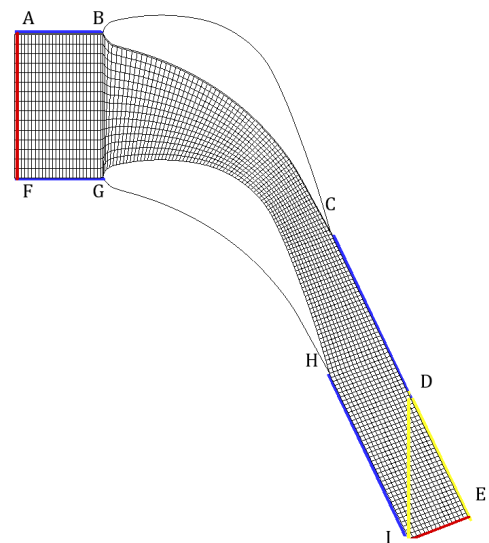


**Fig. 12.** Geometry and the computational grid of mid-section turbines blade



**Table 3.** Comparison of calculated shock wave parameters with the analytical solution (pressure ratio=0.35)

Schemes	Dynamic gas table	AUSM+UP	CUSP	SLAU
Starting point of the shock (m)	1.2523	1.2431	1.2539	1.2539
Position of the end of the shock (m)	1.2523	1.2762	1.2652	1.2652
$M_1$	2.8927	2.8334	2.9919	2.8816
$M_2$	0.4819	0.4701	0.5011	0.5001
$P_{02}/P_{01}$	0.3599	0.415	0.3905	0.3908

**Table 4.** Boundary conditions for 2 cases

Pressure Ratio	Geometry	Condition	Inlet Condition	Pressure Ratio
		$P_{0in}$ (kPa)	$T_{0in}$ (K)	$P_{out}/P_{0in}$
Mid-section	supersonic outlet	172	388	0.48
Mid-section	subsonic outlet	172	388	0.57

### 3.2 Mid-section blade

As mentioned before, to evaluate the performance of the AUSM+UP and SLAU upwind methods in two-dimensional, inviscid flow through stator turbine blades and their comparison with the CUSP artificial dissipation method, the mid-section steam turbine blades are selected firstly. In this research, modeling of the flow is carried out under three different conditions. Boundary conditions for steady-state, adiabatic, inviscid, and two-dimensional flow for two cases are listed in Table 4.

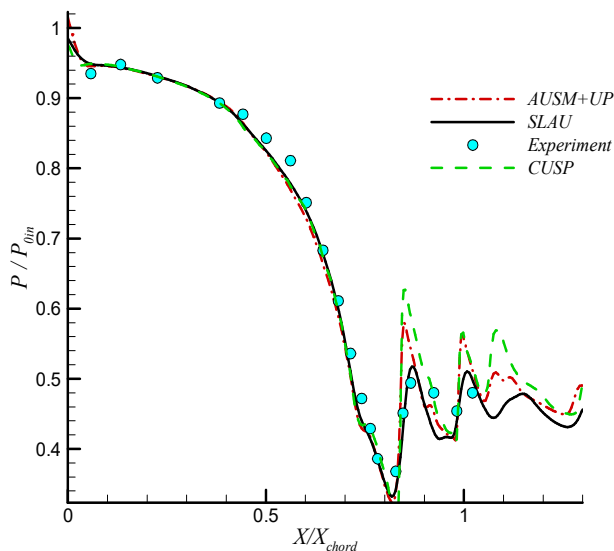
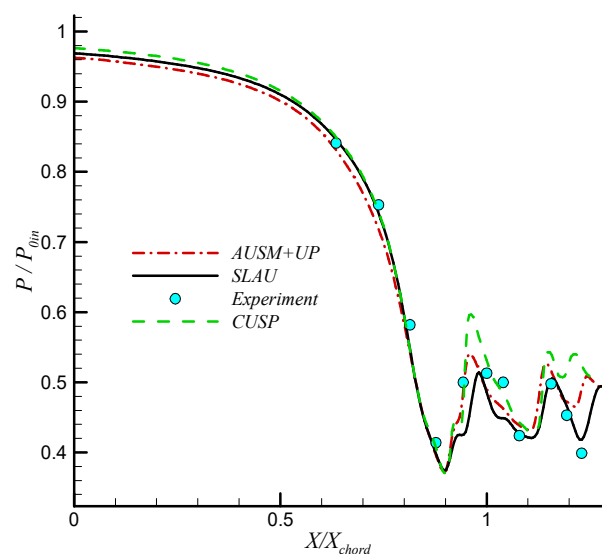
Flow properties such as gas constant and specific heat ratios are used based on steam properties. It should be noted that the small thickness of the boundary layer, due to the expansive nature of the flow in turbines and nozzles, allows inviscid flow assumption [28-31].

Figure 12 shows the geometry of the mid-section turbine blade. In this case, the quasi-orthogonal mesh with 276 cells in the x-direction and 25 cells in the y-direction is used, in which the grid independency is achieved, although, for brevity, the details are not given here.

The blue lines in Fig. 12 show the periodic boundary conditions, and the black lines are the walls. The BC and GH lines represent the pressure side and the suction side, respectively. The inlet and outlet are specified by the red lines and for all cells in a yellow triangle, an alternative solution is to apply to the upper boundary of the yellow triangle the boundary condition of zero-gradient for all the flow variables, which means no change in the triangular region is imposed, e.g. the pressure of these cells will be equal to the backpressure.

The changes in static to inlet stagnation pressure ratio along the blade on the suction and pressure sides and mid passage obtained by the three mentioned schemes in the supersonic condition are shown in Figs. 13-15. It should be noted that the supersonic flow means that the outlet flow downstream of the cascade is supersonic. As shown in these figures, the pressure remains constant until entering the blades but achieves a stagnation point at the inlet of the blade; thus, the pressure of the flow increases, and the velocity decreases. After that, the flow expands along the blade, and the pressure decreases as the velocity increases. The sharp changes in pressure at the end of the blade are due to the aerodynamic shock waves. The target region ( $0.65 < X/X_{chord} < 0.95$ ) is the sensitive and significant shock region on the suction side. The first pressure rise on the suction surface is due to the propagation of the pressure surface shock wave and its collision with the suction surface. After a collision with the suction surface, a reflected shock wave occurs. The next pressure rise on the suction surface represents the aerodynamic shock wave at the trailing edge. As can be seen from these figures, comparing predictions of these schemes with experimental results shows that, in addition to the simplicity of the SLAU scheme, its predictions are in more suitable agreement with experimental data throughout the entire blade.

It can be seen that SLAU has captured the weak shocks correctly, while other schemes have captured the shock waves much stronger. In fact, the SLAU scheme is more reliable in modeling of the flow between steam turbine blades, because it predicts the location and strength of the weak shocks better, while the AUSM+UP and CUSP schemes have considerable deviations in the prediction of the location and strength of the second and third weak shocks.

**Fig. 13.** Distribution of static pressure to inlet stagnation pressure along the blade on the suction side (supersonic outlet)**Fig. 14.** Distribution of static pressure to inlet stagnation pressure along the blade on mid passage (supersonic outlet)

**Table 5.** Percentage of the pressure drop in supersonic outlet condition (supersonic outlet)

Schemes	AUSM+UP	CUSP	SLAU	Ref [28]
Losses (%)	0.76	1.03	1.52	1.5

Table 5 shows the percentage of stagnation pressure drop due to aerodynamic shocks in dry supersonic flow using SLAU, AUSM+UP, and CUSP schemes. It can be seen that the shock-induced losses prediction by the SLAU in the supersonic flow is about 1.52%, which is in good agreement with the values in Table 5 derived from ref [28]. As noted, besides the simplicity of the SLAU method, due to the lack of tuning parameters, because of physical consistency, it provides more consistent results with experimental data throughout the blade. Also, it is superior to the CUSP and AUSM+UP methods in estimating the amount of stagnation pressure drop.

In Figs. 16-17, the changes in static to inlet stagnation pressure ratio along the blade on the suction and pressure sides obtained from SLAU, AUSM+UP, and CUSP schemes in the subsonic condition is illustrated. As can be seen, there is a good agreement between the numerical results and the experimental data. However, the AUSM+UP scheme has flow-dependent parameters such as  $K_u$  and  $K_p$ , which are various in different conditions, and by repeatedly optimizing the value of these parameters are selected. Also, the CUSP scheme has a selective parameter  $q$ , which requires to be determined in different flow conditions according to the available experimental results. Therefore, these schemes are more complicated than the SLAU method and increase the cost of computation.

Table 6 shows the percentage of stagnation pressure drop due to the aerodynamic shocks in a dry subsonic flow using SLAU, AUSM+UP, and CUSP methods.

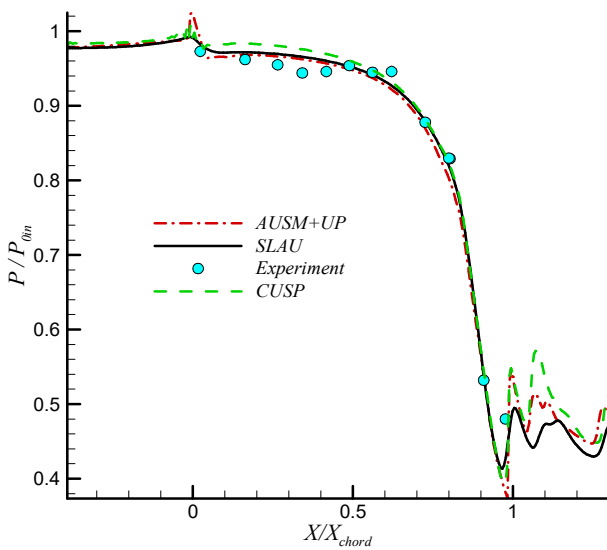


**Fig. 15.** Distribution of static pressure to inlet stagnation pressure along the blade on the pressure side (supersonic outlet)

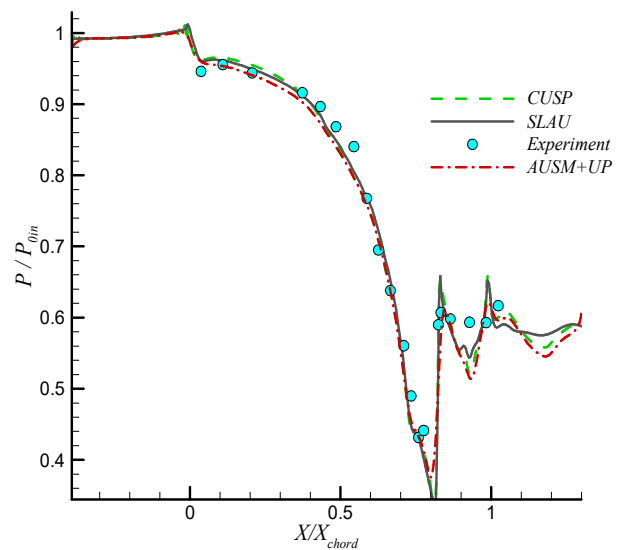


**Fig. 16.** Distribution of static pressure to inlet stagnation pressure along the blade on the suction side (subsonic outlet)

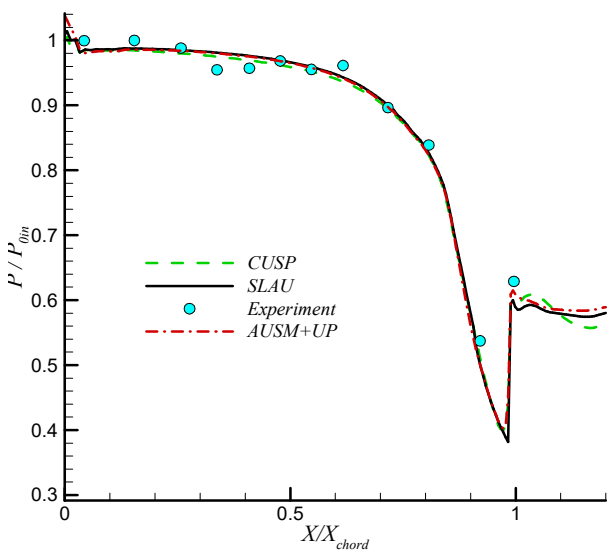


**Fig. 17.** Distribution of static pressure to inlet stagnation pressure along the blade on the pressure side (subsonic outlet)

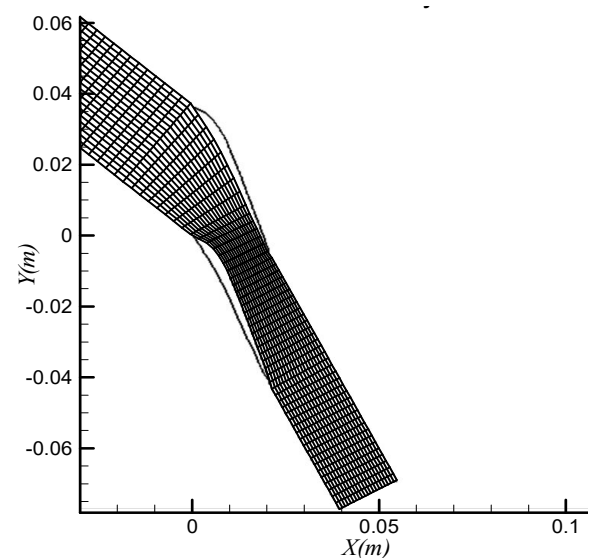


**Fig. 18.** Geometry and the computational grid of tip-section turbines blade



**Table 6.** Percentage of the pressure drop in subsonic outlet condition (subsonic outlet)

Schemes	AUSM+UP	CUSP	SLAU	Ref [28]
Losses (%)	0.32	0.52	0.66	1.1

**Table 7.** Boundary conditions of tip-section turbines blade

Geometry	Condition	Inlet Condition		Pressure Ratio
		$P_{0in}$ (kPa)	$T_{0in}$ (K)	$P_{out}/P_{0in}$
Tip-section	sonic outlet	101.5	388	0.54

A comparison between the current results with those of reference [28] shows that the stagnation pressure drop prediction by the SLAU method is about 0.66%, which predicts the values of the shock-induced losses better than the other two methods.

As noted above, the SLAU scheme, in addition to providing precise results in the preceding sections, in estimating the amount of stagnation pressure drop and simplicity is superior compared to the CUSP and AUSM+UP schemes.

### 3.3 Tip-section blade

In continuation of applying the AUSM+UP, SLAU, and CUSP methods in modeling the flow between turbine blades, the tip section blade is used. Figure 18 illustrates the geometry and computational mesh for the tip-section turbine blade. In this case, the computational grid has 160 cells in the x-direction and 20 cells in the y-direction. Also, mesh independent solution is proven, but it is not presented in the paper for the sake of brevity.

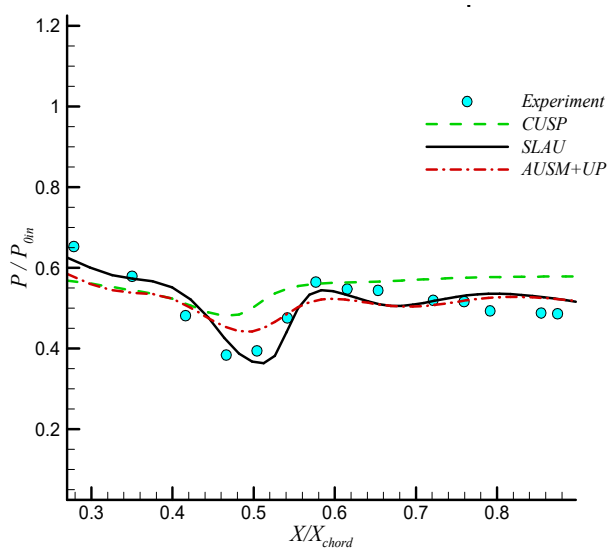


**Fig. 19.** Distribution of static pressure to inlet stagnation pressure along the tip-section blade on the suction side

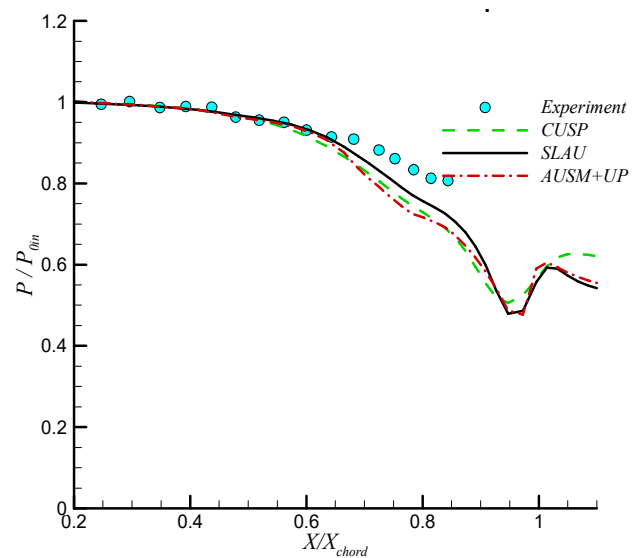


**Fig. 20.** Distribution of static pressure to inlet stagnation pressure along the tip-section blade on the pressure side

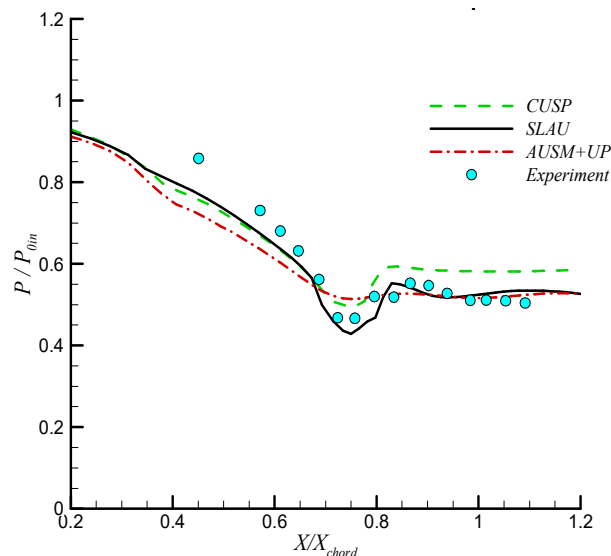


**Fig. 21.** Distribution of static pressure to inlet stagnation pressure along the tip-section blade on the centerline



**Table 8.** Percentage of the pressure drop in the sonic outlet condition of tip-section turbines blade

Schemes	AUSM+UP	CUSP	SLAU	Ref [31]
Losses (%)	0.0	0.0	0.02	0.05

Boundary conditions for steady-state, adiabatic, and inviscid two-dimensional flow for the tip-section blade in transonic outlet conditions are listed in Table 7. Also, flow properties such as gas constant and specific heat ratios are assumed based on steam properties.

In Figs. 19-21, the changes of static to stagnation pressure ratio on the suction and pressure side and the centerline of the transonic outlet flow in the tip-section turbine blade are respectively investigated. The shock wave is detected along the suction side in the  $X/X_{\text{Chord}} = 0.52$ . Comparing the results of these schemes with experimental data [31] shows that the SLAU method compared to the AUSM+UP and the CUSP methods gives more consistent results with the experimental data.

Further, table 8 shows the percentage of stagnation pressure drop in the tip section turbine blade, due to aerodynamic shocks. As it is shown, regarding the complexities of the tip-section turbine blade, the SLAU scheme predicts the stagnation pressure drop value better than the other two methods. In other words, both CUSP and AUSM+UP schemes smear and weaken the shock waves, as they cannot predict the losses for a weak shock wave. These schemes to provide acceptable results need to changes in themselves tuning parameters.

#### 4. Conclusion

Regarding the significance of an effective steam turbine design in different industries, numerous numerical methods have been developed to identify the flow behavior inside the turbine blades. In this research, the performance evaluation of the SLAU, AUSM+UP upwind schemes, and CUSP artificial dissipation scheme has been targeted by developing an in-house code. In the first section, a comparison between the results of the three schemes for one-dimensional, adiabatic, and inviscid flow within the convergent-divergent nozzles with the analytical results revealed a suitable agreement between the SLAU scheme and the analytical solution. Also, the SLAU scheme is more straight forward than the two other schemes and converges at a much higher rate due to the lack of prescribed parameters. Continuing with the research, the AUSM+UP and SLAU upwind schemes and the CUSP artificial dissipation scheme have been used to modeling two-dimensional inviscid flow between the two types of turbine stator blades, namely tip-section and mid-section. The flow is modeled under different outlet conditions downstream of the trailing edge, and the obtained results show that the SLAU scheme has a good agreement with experimental data. Specifically, several subsequent weak shock waves occurred and it was seen that the SLAU scheme predicts the location and strength of these shocks more precisely. Furthermore, the SLAU scheme, dispartate the AUSM+UP and CUSP scheme, does not have tuning and flow-dependent parameters to determine their optimum values in different flows according to the experimental results. So, it has a more straightforward formulation than other all-speed schemes, and using other methods will increase the time of the computation. Therefore, in addition to increasing the accuracy, it can be mentioned as an important advantage of the SLAU method by simplicity and reducing the computation. Moreover, the SLAU scheme is more accurate in predicting the aerodynamic shock losses than the AUSM+UP and CUSP methods, In general, by using the SLAU scheme, the improvement over the prediction of the shock-induced losses in supersonic and subsonic outlet flows are about 30% and 20%, respectively.

#### Author Contributions

F. Ebrahimzadeh Azghadi: Developing the code, Validation, Investigation, Writing the manuscript, M. PasandidehFard: Methodology, Investigation, Supervision, Writing the manuscript, M.R. Mahpeykar: Methodology, Investigation, Supervision. All authors discussed the results, reviewed, and approved the final version of the manuscript.

#### Acknowledgments

Not applicable.

#### Conflict of Interest

The authors declared no potential conflicts of interest with respect to the research, authorship, and publication of this article.

#### Funding

The authors received no financial support for the research, authorship, and publication of this article.

#### Data Availability Statements

The datasets generated and/or analyzed during the current study are available from the corresponding author on reasonable request.

#### References

- [1] Swanson, R.C., Radespiel, R., Turkel, E., On Some Numerical Dissipation Schemes, *Journal of Computational Physics*, 147(2), 1998, 518-544.
- [2] Leonard, B.P., Simple High-accuracy Resolution Program for Convective Modelling of Discontinuities, *International Journal for Numerical Methods in Fluids*, 8(10), 1988, 1291-1318.
- [3] Amanifard, N., Stall Vortex Shedding Over a Compressor Cascade, *International Journal of Engineering*, 18(1), 2005, 9-16.
- [4] Rehman, A., Qamar, S., High Order Finite-volume WENO Scheme for Five-equation Model of Compressible Two-fluid Flow, *Computers & Mathematics with Applications*, 76(11-12), 2018, 2648-2664.
- [5] Jameson, A., Analysis and Design of Numerical Schemes for Gas Dynamics, 1: Artificial Diffusion, Upwind Biasing, Limiters and Their Effect on Accuracy and Multigrid Convergence, *International Journal of Computational Fluid Dynamics*, 4(3-4), 1995, 171-218.
- [6] Liou, M.S., Steffen Jr, C.J., A New Flux Splitting Scheme, *Journal of Computational Physics*, 107(1), 1993, 23-39.
- [7] Liou, M.S., Ten Years in the Making-AUSM-Family, *15th AIAA Computational Fluid Dynamics Conference*, 2001.
- [8] Liou, M.S., A Sequel to AUSM, Part II: AUSM+UP for All Speeds, *Journal of Computational Physics*, 214(1), 2006, 137-170.
- [9] Matsuyama, S., Performance of All-Speed AUSM-Family Schemes for DNS of Low Mach Number Turbulent Channel Flow, *Computers & Fluids*, 91,




2014, 130-143.

- [10] Fořt, J., Fürst, J., Halama, J., Hric, V., Louda, P., Luxa, M., Šimurda, D., Numerical Simulation of Flow Through Cascade in Wind Tunnel Test Section and Stand-alone Configurations, *Applied Mathematics and Computation*, 319, 2018, 633-646.
- [11] Louda, P., Kozel, K., Prihoda, J., Numerical Modelling of Compressible Inviscid and Viscous Flow in Turbine Cascades, *In Proceedings of ALGORITMY*, 2012, 301-310.
- [12] Louda, P., Sváček, P., Fořt, J., Fürst, J., Halama, J., Kozel, K., Numerical Simulation of Turbine Cascade Flow with Blade-fluid Heat Exchange, *Applied Mathematics and Computation*, 219(13), 2013, 7206-7214.
- [13] Pacciani, R., Marconcini, M., Arnone, A., Comparison of the AUSM+UP and Other Advection Schemes for Turbomachinery Applications, *Shock Waves*, 29(5), 2019, 705-716.
- [14] Alakashi, A.M., Basuno, B., Comparison Between Roe's Scheme and Cell-centered Scheme For Transonic Flow Pass Through a Turbine Blades Section. *In IOP Conference Series: Earth and Environmental Science*, 19(1), 2014.
- [15] Singh, R., Holmes, G., Evaluation of an Artificial Dissipation and AUSM Based Flux Formulation: AD-AUSM, *42nd AIAA Fluid Dynamics Conference and Exhibit*, New Orleans, Louisiana, 2012.
- [16] Shima, E., Kitamura, K., On New Simple Low-Dissipation Scheme of AUSM-Family for All Speeds, *47th AIAA Aerospace Sciences Meeting Including the New Horizons Forum and Aerospace Exposition*, 2009.
- [17] Thakur, S.S., Wright, J.A., A Parallel All-Speed Algorithm for High-Resolution Simulations of Turbulent Reacting and Multiphase Flows Using SLAU2 Scheme in a Rule-Based Framework, *AIAA Aerospace Sciences Meeting*, 2018.
- [18] Shima, E., Kitamura, K., Parameter-Free SimpleLow-Dissipation AUSM-Family Scheme for All Speeds, *AIAA Journal*, 49(8), 2011, 1693-1709.
- [19] Soltani, M., Younsi, J., Farahani, M., Investigation of a New Flux Scheme for the Numerical Simulation of the Supersonic Intake Flow, *Proceedings of the Institution of Mechanical Engineers, Part G: Journal of Aerospace Engineering*, 226(11), 2012, 1445-1454.
- [20] Colonia, S., Steijl, R., Barakos, G., Implicit Implementation of the AUSM+ and AUSM+ UP Schemes, *International Journal for Numerical Methods in Fluids*, 75(10), 2014, 687-712.
- [21] Shima, E., Kitamura, K., On AUSM-Family Scheme for All Speeds with Shock Detection for Carbuncle-fix, *19th AIAA Computational Fluid Dynamics*, 2009, 3544.
- [22] Yousefi Rad, E., Mahpeykar, M.R., A Novel Hybrid Approach for Numerical Modeling of the Nucleating Flow in Laval Nozzle and Transonic Steam Turbine Blades, *Energies*, 10(9), 2017, 1285.
- [23] Swanson, R., Radespiel, R., Turkel, E., Comparison of Several Dissipation Algorithms for Central Difference Schemes, *13th Computational Fluid Dynamics Conference*, 1997.
- [24] Hsu, J.M.J., *An Implicit-Explicit Flow Solver for Complex Unsteady Flows*, Stanford University, 2004.
- [25] Yousefi Rad, E., Mahpeykar, M.R., Studying the Effect of Convergence Parameter of CUSP's Scheme in 2D Modelling of Novel Combination of Two Schemes in Nucleating Steam Flow in Cascade Blades, *Numerical Heat Transfer Part B: Fundamentals*, 72, 2017, 325-347.
- [26] Kitamura, K., Hashimoto, A., Reduced Dissipation AUSM-Family Fluxes: HR-SLAU2 and HR-AUSM+-up for High Resolution Unsteady Flow Simulations, *Computers & Fluids*, 126, 2016, 41-57.
- [27] Chen, S.S., Cai, F.J., Xue, H.C., Wang, N., Yan, C., An Improved AUSM-Family Scheme with Robustness and Accuracy for All Mach Number Flows, *Applied Mathematical Modelling*, 77, 2020, 1065-1081.
- [28] Bakhtar, F., Mahpeykar, M.R., Abbas, K., An Investigation of Nucleating Flows of Steam in a Cascade of Turbine Blading-Theoretical treatment, *Journal of Fluids Engineering*, 117(1), 1995, 138-144.
- [29] Bakhtar, F., Zamri M.Y., On the Performance of a Cascade of Improved Turbine Nozzle Blades in Nucleating Steam-Part 3: Theoretical Analysis, *Proceedings of the Institution of Mechanical Engineers, Part C: Journal of Mechanical Engineering Science*, 225(7), 2011, 1649-1671.
- [30] Bakhtar, F., Zamri, M.Y., Rodriguez-Lelis, J.M., A Comparative Study of Treatment of Two-Dimensional Two-Phase Flows of Steam by a Runge-Kutta and by Denton's Methods, *Proceedings of the Institution of Mechanical Engineers, Part C: Journal of Mechanical Engineering Science*, 221(6), 2007, 689-706.
- [31] Bakhtar, F., Mahpeykar, M.R., On the Performance of a Cascade of Turbine Rotor Tip Section Blading in Nucleating Steam Part 3: Theoretical Treatment, *Proceedings of the Institution of Mechanical Engineers, Part C: Journal of Mechanical Engineering Science*, 211(3), 1997, 195-210.

## ORCID iD

Fahimeh Ebrahimzadeh Azghadi  <https://orcid.org/0000-0003-4991-7840>

Mahmoud PasandidehFard  <https://orcid.org/0000-0003-2498-5476>

Mohammad Reza Mahpeykar  <https://orcid.org/0000-0002-3264-5589>



© 2021 Shahid Chamran University of Ahvaz, Ahvaz, Iran. This article is an open access article distributed under the terms and conditions of the Creative Commons Attribution-NonCommercial 4.0 International (CC BY-NC 4.0 license) (<http://creativecommons.org/licenses/by-nc/4.0/>).

**How to cite this article:** Azghadi F.E., PasandidehFard M., Mahpeykar M.R. Performance Investigation of Simple Low-dissipation AUSM (SLAU) Scheme in Modeling of 2-D Inviscid Flow in Steam Turbine Cascade Blades, *J. Appl. Comput. Mech.*, 9(2), 2023, 332-345. <https://doi.org/10.22055/JACM.2021.36513.2857>

**Publisher's Note** Shahid Chamran University of Ahvaz remains neutral with regard to jurisdictional claims in published maps and institutional affiliations.

